

# Investigations into Error Reduction Based FDK

## Algorithms\*

TANG Jie ZHANG Li, XING Yu-xiang, CHEN Zhi-qiang

(Department of Engineering Physics, Tsinghua University, Beijing 100084, China)

**Abstract:** In this paper, we describe the relationship between the reconstruction error and the locus radius. Based on this relationship we formulate our new algorithm. Numerical simulations are done to evaluate its performance and show that the new algorithm can get more accurate reconstruction than algorithms of the same kind. Finally, we discuss the shortcomings of this kind of algorithms.

**Keywords:** computed tomography algorithm; cone-beam reconstruction; circular trajectory

**CLC number:** TP 391.41 R 814.2

**Document code:** A

## 基于FDK算法减小误差的研究

唐杰, 张丽, 邢宇翔, 陈志强

(清华大学工程物理系, 北京, 100084)

**摘要:** 本文介绍了一个重建误差和扫描半径之间的关系, 并在此关系的基础上提出了一种新的基于不同半径的两个同心圆轨道的算法, 利用估算的重建误差改善重建结果。随后进行了数值仿真实验。通过数值模拟实验评价了此算法的性能, 结果表明新的算法能比已有的同类算法更好地估计重建误差, 从而获得更精确的重建结果, 在锥角 $\leq 10^\circ$ 时都能获得相当好的重建结果, 在锥角更大时也能起到很好的改善作用。最后本文讨论了此类算法的局限性。

**关键词:** CT重建算法, 锥束重建, 圆轨道

### 1 Introduction

The well-known Feldkamp algorithm (FDK) for image reconstruction of cone-beam scan in a circular orbit works well when the cone angle is small<sup>[1]</sup>. To increase the cone angle, K. Zeng *et al.* proposed an error reduction based (ERB) method based on FDK reconstructions in 2004<sup>[2]</sup>. In the method, two scans in circular orbits of different radii are used. Then, FDK reconstructions from these two scans are combined to produce a superior image volume by utilizing a relationship between the reconstruction error and the scanning locus radius. They also proposed a half-scan version of this algorithm called HERB method to lower the dosage<sup>[3, 4]</sup>. The algorithm demonstrated improvement in image quality when the cone angle is not very large.

In this report, we present an improved version of ERB-type algorithm to further reduce the reconstruction error. In our scheme, a more accurate relationship between the reconstruction error and the scanning locus radius is utilized to reduce the reconstruction error for the case of a large cone angle. Unfortunately, The new relationship only works fairly well in a certain area. A weighting function is utilized to retain the virtue of original ERB method when out of this area. We refer this new algorithm as Improved Error Reduction Based method, or

---

\*Received data: 2006-01-09. This work is supported by the grant from the National Natural Science Foundation of China(No.10135040/10575059) and the Ph.D. Programs Foundation of Ministry of Education of China(No.20030003074)

IERB method in short. We also present a half scan version of IERB method as HIERB method.

In this paper, we first describe the relationship between the reconstruction error and the locus radius. Then, our new algorithm is formulated and simulations are done to evaluate it numerically in comparison with the classical Feldkamp algorithm and ERB method. Finally, we conclude with a discussion.

## 2 Methods

### 2.1 Relationship between reconstruction error and scanning radius

Although the Feldkamp-type algorithms are rather different from the Grangeat-type algorithms<sup>[5]</sup> in terms of formulation, the Feldkamp-type reconstruction can be equivalent to the Grangeat-type reconstruction in the circular scanning case if the missing data in the Radon space is assumed to be zero<sup>[6]</sup>. Therefore, the Feldkamp algorithm can be analyzed in the Radon space.

The Radon transform is:

$$\mathcal{R}f(\rho, \vec{n}) = \iint_{\vec{r} \in P(\rho, \vec{n})} f(\vec{r}) d\vec{r} \quad (1)$$

Here,  $f(\vec{r})$  is a function on  $R^3$ ,  $P(\rho, \vec{n})$  is a plane defined by  $\vec{r} \cdot \vec{n} = \rho$ .

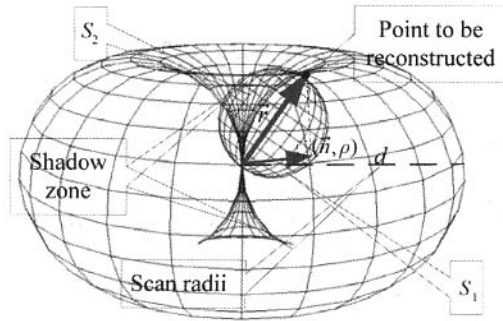


Fig. 1 Shadow zone associated with a circular-orbit cone beam scan

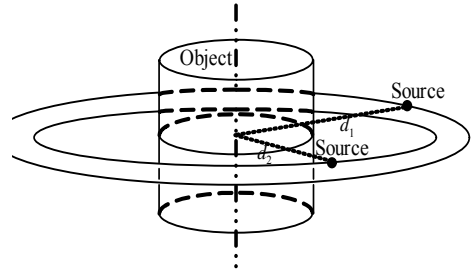


Fig. 2 Scan Geometry

The inverse Radon transform is:

$$f(M) = -\frac{1}{8\pi^2} \int_{S^2} \frac{\partial^2 \mathcal{R}f}{\partial \rho^2} (\vec{r} \cdot \vec{n}, \vec{n}) d\vec{n} \quad (2)$$

Here,  $\vec{n}$  is a vector on the unit sphere  $S^2$ ,  $\vec{r} \cdot \vec{n} = \rho$ .

As shown in Fig. 1, due to the limitation with the imaging geometry, part of Radon information is missing in the cone-beam projection data collected along a scanning circle<sup>[5]</sup>. The missing part forms a shadow zone. Let us assume a spherical object support of radius  $R$  centered at the origin of the reconstruction system. Then, the shadow zone is a pair of cone-shaped regions. In the shadow zone, all the data in Radon space can be assumed to be zero. The inverse 3D Radon transform can be reformulated as a summation of two components:

$$f(\vec{r}) = \left( -\frac{1}{8\pi^2} \int_{S_1} \frac{\partial^2 \mathcal{R}f}{\partial \rho^2} (\vec{r} \cdot \vec{n}, \vec{n}) d\vec{n} \right) + \left( -\frac{1}{8\pi^2} \int_{S_2} \frac{\partial^2 \mathcal{R}f}{\partial \rho^2} (\vec{r} \cdot \vec{n}, \vec{n}) d\vec{n} \right) \quad (3)$$

Here,  $S_1$  denotes the set of points  $(\vec{n}, \rho)$  not included in the shadow zone and  $S_2$  denotes the set of points  $(\vec{n}, \rho)$  included in the shadow zone. Let  $f_{\text{error}}(\vec{r})$  denote the reconstruction error from the FDK method. From Zeng's work, we know that, when the cone angle is small (i.e. the shadow zone is very small compared with the whole object), it is approximately true that<sup>[7]</sup>:

$$f_{\text{error}}(\vec{r}) = \text{const}(\vec{r}, f(\vec{r})) \times S_2 \quad (4)$$

That means, the reconstruction error is approximately proportional to  $S_2$ .

Let  $d$  denote the scanning locus radius and  $(x_m, y_m, z_m)$  the point to be reconstructed. The  $S_2$  can be computed as following<sup>[8]</sup>:

$$\text{Let } \rho_m = \sqrt{x_m^2 + y_m^2}, r_m = \sqrt{x_m^2 + y_m^2 + z_m^2} / 2,$$

$$x_{p1} = \frac{dz_m^2}{(d - \rho_m)^2 + z_m^2}, z_{p1} = \frac{dz_m(d - \rho_m)}{(d - \rho_m)^2 + z_m^2}, \quad x_{p2} = \frac{-dz_m^2}{(d + \rho_m)^2 + z_m^2}, z_{p2} = \frac{dz_m(d + \rho_m)}{(d + \rho_m)^2 + z_m^2}$$

$$\phi_{\max} = \arctan \left| \frac{z_{p1} - z_m/2}{x_{p1} - \rho_m/2} \right|, \phi_{\min} = \arctan \left| \frac{z_{p2} - z_m/2}{x_{p2} - \rho_m/2} \right|$$

$$r_1 = \frac{\rho_m}{2}, r_2 = \sqrt{\frac{\rho_m^2}{4} + \frac{z_m^2}{4}} \cos \phi, r_3 = \frac{d}{2} - \sqrt{\frac{d^2}{4} - \left( \frac{z_m}{2} + \sqrt{\frac{\rho_m^2}{4} + \frac{z_m^2}{4}} \sin \phi \right)^2}, \quad l(\phi) = \pi r_2 \cdot 2 \arccos \frac{r_1^2 + r_2^2 - r_3^2}{2r_1r_2}$$

$$\text{When } x_{p1} \leq \rho_m / 2, \text{ we have} \quad S_2 = \int_{\phi_{\min}}^{\phi_{\max}} l(\phi) r_m d\phi \quad (5)$$

$$\text{When } x_{p1} > \rho_m / 2, \text{ we have} \quad S_2 = \int_{\phi_{\min}}^{\phi_{\max}} l(\phi) r_m d\phi + 2\pi r_m (z_m / 2 + r_m - z_{p1}), \quad (6)$$

## 2.2 Reconstruction method

In our imaging, scans in two concentric circular orbits of different radii,  $d_1$  and  $d_2$ , are done as shown in Fig. 2. Two reconstructions from these two scans are obtained using the standard Feldkamp algorithm. Let  $f_{\text{FDK}, d1}(\vec{r})$  denote the reconstruction from the orbit of radius  $d_1$ , and  $f_{\text{FDK}, d2}(\vec{r})$  denote the reconstruction from the orbit of radius  $d_2$ . Let  $f(\vec{r})$  denote the true value. From our previous deduction we have:

$$f(\vec{r}) = f_{\text{FDK}, d1}(\vec{r}) + \text{const}(\vec{r}, f(\vec{r})) \times S_2(d_1, \vec{r}) \quad (7)$$

$$f(\vec{r}) = f_{\text{FDK}, d2}(\vec{r}) + \text{const}(\vec{r}, f(\vec{r})) \times S_2(d_2, \vec{r}) \quad (8)$$

By combining (7) and (8), we get our reconstruction as:

$$f(\vec{r}) = f_{\text{FDK}, d1}(\vec{r}) + \frac{f_{\text{FDK}, d1}(\vec{r}) - f_{\text{FDK}, d2}(\vec{r})}{S_2(d_2, \vec{r}) - S_2(d_1, \vec{r})} S_2(d_1, \vec{r}) \quad (9)$$

In this way, the FDK reconstructions from two scans are combined to produce a superior image volume.

To perform such a method, we should do as following:

- 1) Reconstruct two volume data  $f_{\text{FDK}, d_1}(\vec{r})$  and  $f_{\text{FDK}, d_2}(\vec{r})$  from two set scan data under different radius;
- 2) Compute the corresponding  $S_2(d_2, \vec{r})$  and  $S_2(d_1, \vec{r})$  of the reconstruction voxel position  $\vec{r}$  by (5) and (6).
- 3) Compute the reconstruction  $f(\vec{r})$  by (9).

### 2.3 Weighting function

We should point out that this method is based on (4), which assume the shadow zone is very small compared with the whole object. When the cone angle increases, the shadow zone become fairly large so that we can't get a better reconstruction by (9). On the other hand, it can be observed that the ERB method doesn't suffer much when the cone angle increases. We believe that is because the ERB method works not only on the compensation of the incomplete radon data. So we applied a weighting function to retain this virtue of ERB method.

$$\text{Let: } c(d_1, d_2, \vec{r}) = \frac{S_2(d_1, \vec{r})}{S_2(d_2, \vec{r}) - S_2(d_1, \vec{r})} \quad (10)$$

And (9) can be reformed as:

$$f(\vec{r}) = f_{\text{FDK}, d_1}(\vec{r}) + c(d_1, d_2, \vec{r})[f_{\text{FDK}, d_1}(\vec{r}) - f_{\text{FDK}, d_2}(\vec{r})] \quad (11)$$

Then we can consider  $c$  as a weighing function, and the problem becomes how to choose this weighting function. In ERB method  $c$  is a constant during a reconstruction process. And the whole reconstruction volume get a uniform correction. But when use our new relationship,  $c$  decreases sharply when the cone angle increases to about  $10^\circ$ . Then the reconstruction can't get corrected properly. We defined points inside this boundary as  $R_{\text{inner}}$  and points out of this boundary as  $R_{\text{outer}}$ . We selected  $c$  as following:

$$c(d_1, d_2, \vec{r}(x, y, z)) = \begin{cases} \frac{S_2(d_1, \vec{r})}{S_2(d_2, \vec{r}) - S_2(d_1, \vec{r})}, \vec{r} \in R_{\text{inner}} \\ \frac{d_2^2 + z^2}{d_1^2 - d_2^2}, \vec{r} \in R_{\text{outer}} \end{cases} \quad (12)$$

### 2.4 Half-scan Version Algorithms

Half-scan can decrease the radiation dose and scanning time. By inserting the Parker weighting formula<sup>[9]</sup> into the Feldkamp algorithm<sup>[1]</sup>, we can immediately obtain a half-scan version of the Feldkamp algorithm and our HIERB method.

## 3 Numerical Simulation

In the numerical simulation, the low contrast 3D Shepp- Logan phantom was used to evaluate the IERB algorithm against the Feldkamp-type algorithms, which has an ellipsoid support with half axes of 88.32 mm, 115.2 mm and 117.76 mm along the x-, y- and z-axis, respectively. Noise-free cone beam projections were analytically synthesized on a flat-panel detector. The simulation parameters are summarized in Table 1. For convenience, the detector was placed at the rotation center.  $S_2$  was computed by numerical integration according to (5) and (6). In half-scan version algorithms, only projections between 0 and  $\pi + 2 \times \text{FanAngle}$  were used.

Representative reconstruction images of the slice parallel to rotation axis at position  $Y = -31.5\text{mm}$  from different algorithms are shown in Fig. 3. Vertical profiles at position  $X = 0.5\text{mm}$  of the slice and its zoomed-in are plotted in Fig. 4. Horizontal profiles at position  $Z = 58.5\text{mm}$  of the slice and its zoomed-in are plotted in Fig. 5. Zoomed-in profiles at the same position in half-scan reconstructions are plotted in Fig. 6. It can be ob-

served that the traditional Feldkamp-type reconstructions suffer from a significant intensity dropping away from the mid-plane, which is a well-known drawback of the Feldkamp algorithm. ERB suppressed this sort of artifacts, even for a fairly large cone angle several times larger than that with the traditional Feldkamp-type reconstruction for a similar image quality. Compared with ERB our IERB reconstruction improved the image quality further and accords better with the true value. But two obvious boundaries can be observed in IERB reconstruction. A smoother weighting function may eliminate this sharp border, and it will be done in the future. In the half-scan reconstructions, IERB method is similar to ERB method, and no obvious improvement can be observed.

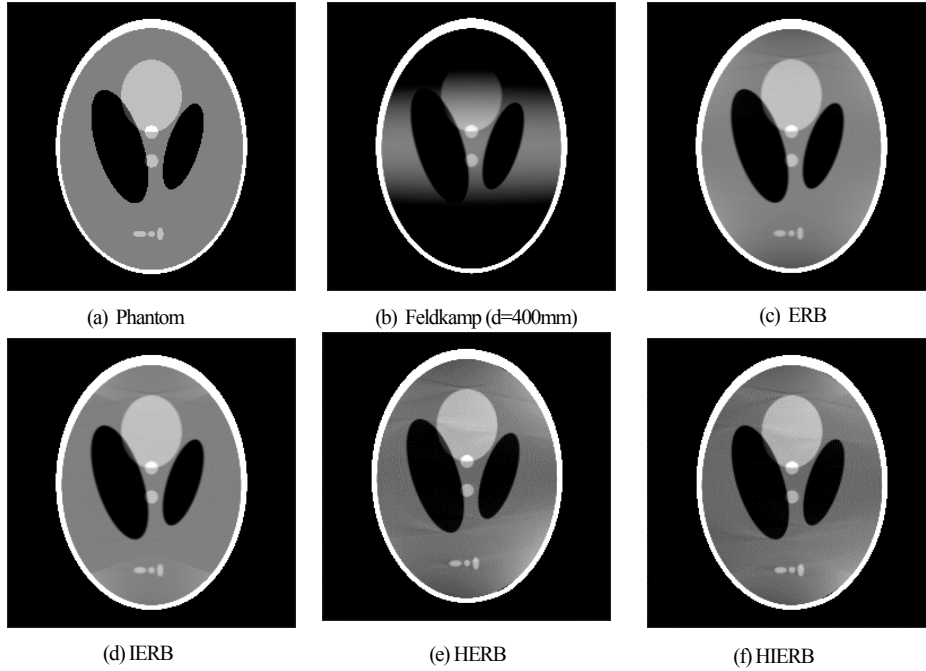


Fig. 3 3D Shepp-Logan phantom and reconstructions for the slices at  $Y = -31.5\text{mm}$ .

The grayscale was mapped to  $[0,255]$  from the original interval  $[1.00,1.04]$ .

TABLE 1

SIMULATION PARAMETERS FOR EVALUATION OF THE IERB ALGORITHM.

DISTANCE MEASURES ARE IN MILLIMETER

Scanning radius(mm)	$d_1$	300
	$d_2$	400
Cone angle (degree)	$d_1$	$\arctan(128/300) = 23^\circ$
	$d_2$	$\arctan(128/400) = 18^\circ$
Fan angle (degree)	$d_1$	$\arctan(128/300) = 23^\circ$
	$d_2$	$\arctan(128/400) = 18^\circ$
Number of projections		360
Detector size (Height $\times$ Width)(mm)		$256 \times 256$
Detector number		$256 \times 256$
Reconstruction grid ( $\text{mm}^3$ )		$256 \times 256 \times 256$

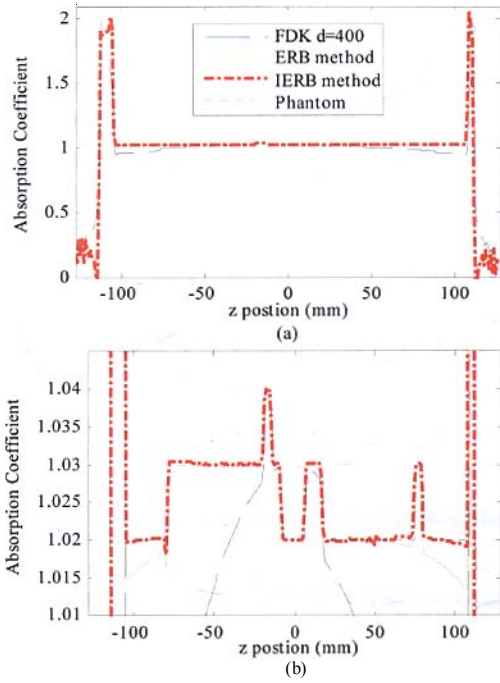


Fig. 4 profiles along the vertical line at  $x = 0.5mm$  in the selected slice of the phantom and full-scan reconstructions.

(a) Entire profiles, and (b) zoom in the magnitude of the profiles

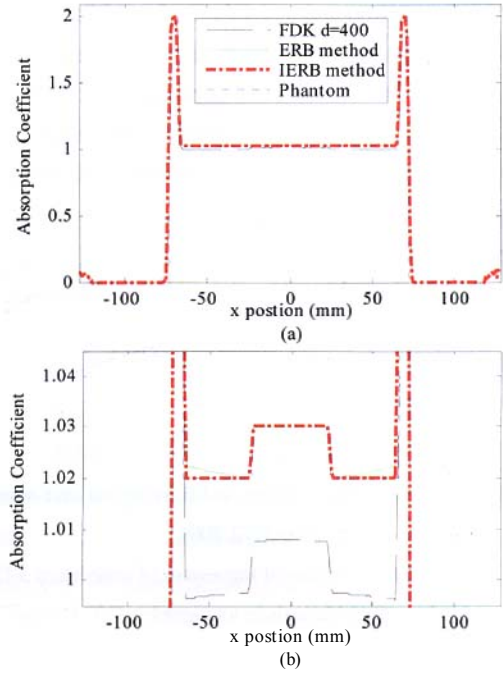


Fig. 5 profiles along the horizontal line at  $Z = 58.5mm$  in the selected slice of the phantom and full-scan reconstructions.

(a) Entire profiles, and (b) zoom in the magnitude of the profiles.

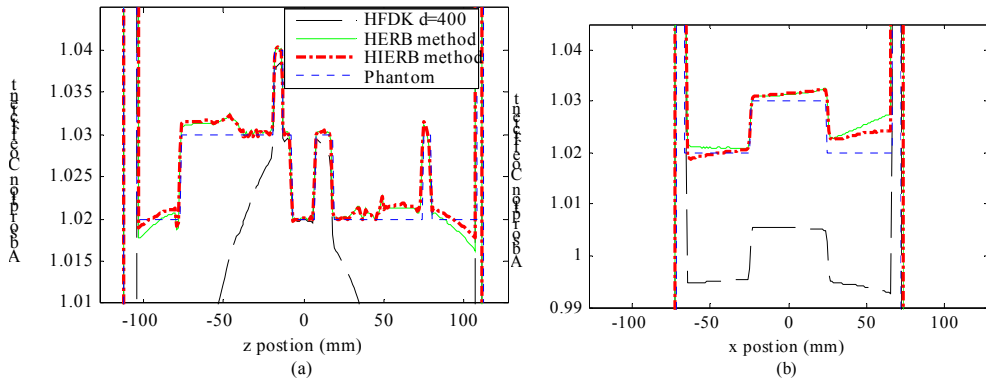


Fig. 6 profiles along the vertical line at  $x = 0.5mm$  in the selected slice of the phantom and full-scan reconstructions.

(a) Entire profiles, and (b) zoom in the magnitude of the profiles.

## 4 Discussion

We present our method to improve the ERB method proposed by Zeng so that more accurate reconstruction can be achieved. The method bears some similarity to the ERB method, but differ primarily in the computation of the area of shadow zone in the Radon domain.

In the IERB full-scan reconstruction, the pixel value inside the valid area is very close to the true value. For voxels out of the valid area, IERB method works slightly better than ERB method.

In the half-scan reconstructions, IERB method is similar to ERB method. We believe that is because both of them are extrapolation methods. In two half-scan reconstructions, the angle range of backprojection varies, which causes that the correction is not so perfect as in full-scan.

IERB method uses the same theory as ERB method but computes the area of shadow zone in the Radon domain more accurately. However, the linear relationship between the area of shadow zone in the Radon domain and the exact error from FDK could break in some cases. More thorough research shall be done on this aspect.

### References :

- [1] I. A. Feldkamp, L. C. Davis, and J. W. Kress. Practical Cone-beam Algorithm.[J]. Opt.Soc.Am.A, vol. 1, pp. 612-619, 1984.
- [2] Z. Kai, C. Zhiqiang, Z. Li, and Z. Ziran. Cone beam reconstruction algorithm based on two concentric circles[J]. Journal of Tsinghua University (Science and Technology), vol. 44, pp. 725-7, 2004.
- [3] K. Zeng, Z. Chen, L. Zhang, and G. Wang. A half-scan error reduction based algorithm for cone-beam CT[J]. Journal of X-Ray Science and Technology, vol. 12, pp. 73-82, 2004.
- [4] K. Zeng, Z. Chen, L. Zhang, and G. Wang. An error-reduction-based algorithm for cone-beam computed tomography[J]. Med. Phys., vol. 31, pp. 3206-3212, 2004.
- [5] P. Grangeat. Mathematical framework of cone beam 3-D reconstruction via the first derivative of the radon transform[M]. in Mathematical Methods in tomography, G.T. Herman, A.K. Louis, and F. Natterer, Eds.: pp. 66-97, Springer Verlag, New York, 1990.
- [6] M. Defrise and R. Clack. Cone-beam reconstruction algorithm using shift-variant filtering and cone-beam backprojection[J]. IEEE Transactions on Medical Imaging, vol. 13, pp. 186-195, 1994.
- [7] Z. Kai, C. Zhiqiang, Z. Li, and Z. Ziran. The Study of the Relationship between the Circular Orbit Cone Beam Reconstruction Error and the Cone Angle[J]. Computerized Tomography Theory And Applications, vol. 12, pp. 9-16, 2003.
- [8] J. Tang, L. Zhang, Y. Xing, and W. Gao. Data incompleteness in radon space in circular cone-beam reconstruction[J]. Journal of Tsinghua University Sci & Tech, in press.
- [9] D. L. Parker. Optimization of Short scan Convolution Reconstruction in Fan Beam CT[C]. presented at International Workshop on Physics and Engineering in Medical Imaging., Pacific Grove, CA, USA, 1982.

### Brief introduction for authors :

**TANG Jie**, male, is a PhD candidate of the Dept. of Engineering Physics, Tsinghua University. His main researches are X-ray imaging physics, CT imaging mathematics and their applications. Address: Dept. of Engineering Physics, Tsinghua University, Beijing, China (100084). Tel: 8610-62780909-86092. Email: tangjie35@tsinghua.org.cn.

**ZHANG Li**, female, is an associate professor of the Dept. of Engineering Physics, Tsinghua University. Her research is X-ray imaging systems and technology, image data correction, image processing and pattern recognition.

**XING Yuxiang**, female, is a lecturer of the Dept. of Engineering Physics, Tsinghua University. Her research is X-ray imaging systems and technology, image data correction, 3D imaging reconstruction.

**CHEN Zhiqiang**, male, is an associate professor of the Dept. of Engineering Physics, Tsinghua University. His research is X-ray imaging systems and technology, 3D imaging reconstruction, image processing and image visualization.